AGU PUBLICATIONS

Geophysical Research Letters

RESEARCH LETTER

10.1002/2014GL061896

Key Points:

- Near-cloud aerosols around the Azores are studied using CALIPSO lidar data
- Data show that cloud fraction affects apparent aerosol enhancement near clouds
- Cloud fraction variations inflate near-cloud changes in composite statistics

Correspondence to:
W. Yang,
Weidong.Yang@nasa.gov

Citation:
Yang, W., A. Marshak, T. Várnai, and R. Wood (2014), CALIPSO observations of near-cloud aerosol properties as a function of cloud fraction, *Geophys. Res. Lett.*, *41*, 9150–9157, doi:10.1002/2014GL061896.

Received 25 SEP 2014
Accepted 19 NOV 2014
Accepted article online 22 NOV 2014
Published online 16 DEC 2014

CALIPSO observations of near-cloud aerosol properties as a function of cloud fraction

Weidong Yang[1,2], Alexander Marshak[2], Tamás Várnai[2,3], and Robert Wood[4]

[1]Goddard Earth Sciences Technology and Research, Universities Space Research Association, Columbia, Maryland, USA, [2]NASA Goddard Space Flight Center, Greenbelt, Maryland, USA, [3]Joint Center for Earth System Technology, University of Maryland at Baltimore County, Baltimore, Maryland, USA, [4]Department of Atmospheric Sciences, University of Washington, Seattle, Washington, USA

Abstract This paper uses spaceborne lidar data to study how near-cloud aerosol statistics of attenuated backscatter depend on cloud fraction. The results for a large region around the Azores show that (1) far-from-cloud aerosol statistics are dominated by samples from scenes with lower cloud fractions, while near-cloud aerosol statistics are dominated by samples from scenes with higher cloud fractions; (2) near-cloud enhancements of attenuated backscatter occur for any cloud fraction but are most pronounced for higher cloud fractions; (3) the difference in the enhancements for different cloud fractions is most significant within 5 km from clouds; (4) near-cloud enhancements can be well approximated by logarithmic functions of cloud fraction and distance to clouds. These findings demonstrate that if variability in cloud fraction across the scenes used for composite aerosol statistics is not considered, a sampling artifact will affect these statistics calculated as a function of distance to clouds. For the Azores region data set examined here, this artifact occurs mostly within 5 km from clouds and exaggerates the near-cloud enhancements of lidar backscatter and color ratio by about 30%. This shows that for accurate characterization of the changes in aerosol properties with distance to clouds, it is important to account for the impact of changes in cloud fraction.

1. Introduction

Aerosol-cloud interactions can induce significant changes in the optical and microphysical properties of clouds and aerosols and are therefore highly important for understanding solar radiative forcing and climate change. In examining aerosol-cloud interactions, many observational studies have found positive correlations between cloud fraction and Aerosol Optical Depth (AOD), or solar reflectance, and/or lidar backscatter [e.g., *Ignatov et al*., 2005; *Loeb and Manalo-Smith*, 2005; *Matheson et al*., 2005; *Zhang et al*., 2005; *Kaufman and Koren*, 2006; *Koren et al*., 2007; *Loeb and Schuster*, 2008; *Su et al*., 2008; *Redemann et al*., 2009; *Chand et al*., 2012]. Other studies found that clear areas near clouds have higher lidar backscatter (or solar reflectance) values than areas far from clouds do, thus forming areas called “twilight zone” or “transition zone” [e.g., *Platt and Gambling*, 1971; *Lu et al*., 2003; *Charlson et al*., 2007; *Koren et al*., 2007]. Such zones are characterized by a gradual increase in the reflected signal as the measurements approach a cloud [*Tackett and Girolamo*, 2009; *Várnai and Marshak*, 2011, 2012; *Yang et al*., 2012; *Várnai et al*., 2013]. Physically, such zones are thought to contain aerosols swollen in the humid air that surrounds clouds, aerosols generated or processed in the clouds, and undetected small and/or thin cloud pieces [e.g., *Hoppel et al*., 1986; *Clarke et al*., 2002; *Su et al*., 2008; *Koren et al*., 2008, 2009; *Bar-Or et al*., 2010, 2011, 2012].

In addition, it was found that instrumental limitations [*Qiu et al*., 2000], cloud contamination [e.g., *Zhang et al*., 2005], and three-dimensional (3-D) solar radiative processes [e.g., *Wen et al*., 2007; *Marshak et al*., 2008; *Kassianov and Ovtchinnikov*, 2008] in cloudy environments can also contribute significantly to the apparent enhancements observed near clouds. Analysis of the contributing factors in the near-cloud enhancements is needed to help better understand both cloud-aerosol interactions and the direct radiative effect of aerosols [e.g., *Várnai et al*., 2013].

Studies of aerosol near-cloud behavior often involve statistics taken from large data sets that cover large areas and a long time span. For example, in a global yearlong data set, *Várnai and Marshak* [2012] found an anticorrelation between median distance to cloud and cloud fraction, though they also noted that cloud structure also influences the distribution of distance to cloud. One may argue that far-from-clouds clear-sky regions can occur only in areas with low cloud fractions while the statistics of close-to-clouds regions are

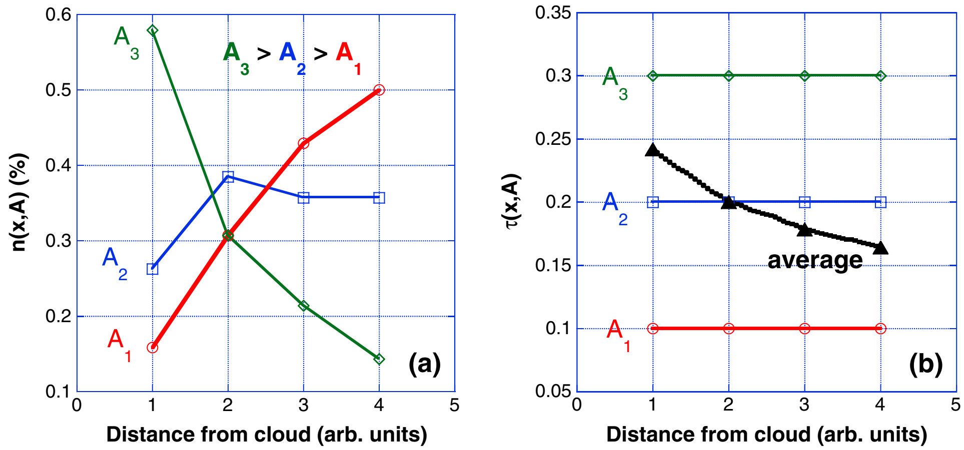

Figure 1. Schematic illustration of the potential effect of sampling on the averaged aerosol optical thickness (AOT) as a function of distance to cloud, x. (a) Probability density function $n(x,A)$ [$\int n(x, A)\mathrm{d}A = 1$] for three cloud fractions $A_1 < A_2 < A_3$. (b) Average AOT, [$\bar{\tau}(x) = \int \tau(x, A)n(x, A)\mathrm{d}A$] assuming AOT for each cloud fraction is constant: $\tau(x,A_1) = 0.1$, $\tau(x,A_2) = 0.2$, $\tau(x,A_3) = 0.3$.

likely to be strongly influenced by areas with higher cloud fractions. Therefore, AOD (as well as reflectance or lidar backscatter) may be higher close to clouds than far from clouds simply because of the well-documented positive correlations between AOD and cloud fraction [e.g., *Loeb and Manalo-Smith*, 2005; *Chand et al.*, 2012]. As a result, the statistically increasing scattering enhancement as clouds are approached could potentially merely be a consequence of these correlations, rather than reflecting any physical changes near clouds.

The above argument can be illustrated through a simple example. We consider a data set in which aerosol samples are obtained in three regions with different cloud fractions A_1, A_2, and A_3, and we assume that $A_3 > A_2 > A_1$ (Figure 1a). Let us further assume that clear-sky AODs in each region remain constant with respect to distance to clouds and have values of τ_1, τ_2, and τ_3 for each of the regions with A_1, A_2, and A_3, respectively (Figure 1b). The assumption that $\tau_3 > \tau_2 > \tau_1$ while $A_3 > A_2 > A_1$ is well consistent with the observed correlation between AOD and cloud coverage.

Combining data from all regions together, the average AOD (symbol $\bar{\tau}$) at distance x from clouds is the weighted sum of $\tau(x, A)$ over all cloud fraction (A) values, i.e.,

$$\bar{\tau}(x) = \int_0^1 \tau(x, A)n(x, A)\mathrm{d}A. \tag{1}$$

Here the weight $n(x, A)$ is the ratio of the number of samples with A at x to the total number of all samples with all As at x, and so $\int_0^1 n(x, A)\mathrm{d}A = 1$. As *Várnai and Marshak* [2012] found some anticorrelation between distance to cloud and cloud fraction, we can expect to find progressively more samples with high cloud fraction as we approach clouds. Therefore, in this simple example, it is plausible to assume that weights of given cloud fractions vary as shown schematically in Figure 1a. In Figure 1a $n(x, A_1)$ is an increasing function of x while $n(x, A_3)$ is a decreasing one. Because low cloud fraction is associated with low AOD, the changes in the sample weights lead to an apparent enhancement of $\bar{\tau}$ closer to clouds (black curve in Figure 1b). This reveals that statistical results may behave differently from our initial assumption of distance-independent, constant AOD for individual scenes. In the following, we call the apparent enhancement described above as *sampling effect/sampling artifact* for the reason that it is induced by variation of sampling weights of cloud fractions, instead of the variation of near-cloud aerosol properties.

This raises the questions: *What is the true statistical near-cloud behavior? Do the enhancements observed in earlier studies come entirely from this effect?* To address these questions, we first analyze the samples' cloud fraction-dependent features as a function of distance to cloud using a CALIPSO data set over the Atlantic Ocean. Next, we examine the near-cloud behaviors of aerosols for various cloud fractions. Finally, we introduce a method for studying near-cloud aerosol properties using satellite observations and estimate the fraction of enhancements due to the statistical cloud fraction-sampling effect.

2. Data and Methodology

In this study we analyze data from a large region over the Atlantic Ocean near the Azores (25°–45°N, 20°–37°W). This region is well suited for this study because it is rich in low-level marine boundary layer clouds types and cloud fractions and is ideal site for studying interactions between cloud, aerosol, and precipitation [e.g., *Wood*, 2009; *Rémillard et al*., 2012; *Dong et al*., 2014; *Wood et al*., 2014].

We examine this region using data from the CALIOP (Cloud-Aerosol Lidar with Orthogonal Polarization) lidar on board the CALIPSO (Cloud Aerosol-Lidar and Infrared Path finder Satellite Observations) satellite, which was launched in 2006 [e.g., *Winker et al*., 2007]. CALIOP provides range-resolved cloud and aerosol data along its track, including attenuated total lidar backscatter at 532 nm and 1064 nm and perpendicularly polarized lidar backscatter at 532 nm. CALIOP operational algorithms (currently in version 3) use this data along with altitude and latitude information for feature identification and classification [*Liu et al*., 2009; *Omar et al*., 2009].

Similarly to earlier studies [e.g., *Várnai and Marshak*, 2011, 2012; *Yang et al*., 2012], we reduce the noise due to background illumination and sampling by using only nighttime data and by combining observations from a three year period (2006.6.21-2009.6.21) over the entire study region.

In this study, we examine the 532 nm attenuated total lidar backscatter coefficient β (the ratio of vertically integrated backscatter within an aerosol layer over layer thickness) and the attenuated total color ratio χ (ratio of total backscatter at 1064 nm over that at 532 nm) at a horizontal resolution of 333 m. The backscatter coefficient is used for examining variations in the optical density of aerosol layers, while the color ratio is related to changes in the size of spherical particles [*Liu et al*., 2000, 2004; *Cattrall et al*., 2005; *Omar et al*., 2005]. To be consistent with earlier studies [*Várnai and Marshak*, 2011, 2012; *Yang et al*., 2012], we examine aerosol properties in cloud-free columns as a function of distance to the nearest cloud edge—the closest point where a cloud is detected in the 0.333 km or 1 km cloud mask. While the 5 km resolution cloud mask is not used for defining the nearest cloud edge, aerosol data are used only when the 5 km cloud mask (most sensitive to thin clouds) also indicates a fully cloud-free column at all altitudes. Also, we use aerosol data only if the nearest cloud is of liquid water phase with a cloud top below 3 km and if the top of the aerosol layer is below 5 km. Moreover, we exclude data from clear-sky segments shorter than 3 km in order to reduce the amount of data possibly contaminated by undetected clouds. To further reduce the influence from undetected clouds, aerosol data are used only if a particle layer is identified as an aerosol layer with high confidence [*Liu et al*., 2009], with CAD (cloud-aerosol discrimination) values larger than 70. (Additional tests showed that using higher CAD thresholds does not change the basic observed behaviors and our conclusions.)

In this paper, we define cloud fraction as the ratio of the number of 0.333 km cloudy profiles (with clouds in either the 0.333 km or 1 km resolution cloud mask) to the total number of 0.333 km profiles within 15 km from it. Since CALIOP can only detect clouds and aerosols along the 1-D track, clouds off the track are unknown and can cause uncertainties in estimating the true distance to clouds and cloud fraction [e.g., *Astin et al*., 2001]. However, the cloud fractions estimated based on 1-D tracks and 2-D images should be statistically similar; as a result, the cloud fraction-dependent features found in 1-D can be a good approximation of the features in 2-D. Finally, *Várnai and Marshak* [2012] found that near-cloud behaviors are highly correlated when considering 1-D or 2-D distances to clouds.

3. Results

The distribution of the total number of aerosol samples $N(x, A)$ as a function of distance to clouds x and cloud fraction A is shown in Figure 2. Figure 2a indicates that the sample number distributions vary with cloud fraction in a way that depends on how close the samples are to clouds: At farther distances, samples are distributed over a narrow range of small cloud fractions (see the purple curve); while at closer distances, samples are from a much wider cloud fraction range and mostly from higher cloud fractions of 0.3–0.5 (e.g., the red curve). This behavior is consistent with the assumptions used in the introduction

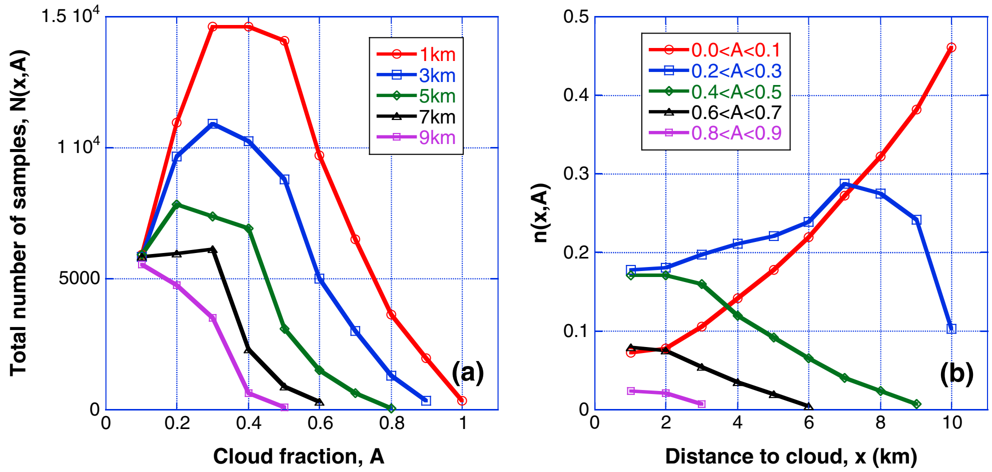

Figure 2. Sample numbers used in the analysis. (a) Total number of samples, $N(x,A)$, for each distance to cloud x, as a function of cloud fraction A. (b) Probability density function $n(x,A) = N(x,A)/\int N(x, A)\mathrm{d}A$ as a function of distance to cloud.

(Figure 1a). Figure 2b shows the way the sample fraction ($n(x, A)$ in equation (1)) changes with distance to cloud for various ranges of cloud fraction. The plot shows that for low cloud fractions (red curve) sample fractions increase dramatically with distance, while for high cloud fractions (e.g., black curve) sample fractions decrease with distance. We note that this behavior is qualitatively similar to the one assumed in Figure 1a. These features arise from the fact that far-from-cloud samples are more easily found in areas of smaller cloud fractions than larger ones.

The near-cloud properties observed at specific cloud fractions are shown in Figure 3. The most important findings are as follows. (1) The enhancements of near-cloud backscatter and color ratio occur for *all* cloud fractions and are most pronounced for higher cloud fraction values, as shown in Figures 3a and 3b. This feature indicates that the mechanisms causing the near-cloud enhancements (such as aerosol humidification and cloud contamination) are present in all clear-sky conditions but are most prominent in high cloud fraction cases. (2) At a given distance away from cloud, both the attenuated total backscatter coefficient β and color ratio χ are increasing functions of cloud fraction and are more sensitive to cloud fraction at closer distances (Figures 3c and 3d). In contrast, the positive correlations of backscatter coefficient and color ratio with cloud fraction are not significant at larger distances to clouds ($> \sim 5$ km). This indicates that clouds have a strong influence on their surroundings, but the range of influence may be limited to about 5 km, at least for this data set. (3) As indicated by the high regression coefficients R, the enhancements in near-cloud aerosol properties can be well approximated by the logarithmic functions, i.e.,

$$\beta(x, A) \approx a_1(A) - b_1(A)\cdot \log(x) \tag{2}$$

and

$$\chi(x, A) \approx a_2(A) - b_2(A)\cdot \log(x) \tag{3}$$

where, in this study, A ranges from 0.1 to 1 and x is the dimensionless distance to clouds normalized by the resolution of 1 km, with $x \geq 1$. Let us analyze the trend in coefficients a and b in the logarithmic approximation of the attenuated total backscatter coefficient $\beta(x, A)$ (see equation (2) and Figures 3a and 3c). (The coefficients for the attenuated total color ratio $\chi(x, A)$ behave similarly (Figures 3b and 3d)). First, $a_1(A) = \beta(x = 1,A)$ describes the near-cloud behavior while $b_1(A)$ is the degree of dependence on the distance to clouds; both are functions of cloud fraction A (Figure 3a). As expected, both a_1 and b_1 are increasing functions of A, i.e., the larger A the bigger β near clouds and the stronger changes in β with the distance from cloud. Note that for the smallest cloud fraction (red curve), a_1 and b_1 are both the smallest and show the weakest dependence on distance from cloud.

Figure 3c shows that the attenuated backscatter $\beta(x, A)$ as a function of A can be also well approximated by a logarithmic function,

$$\beta(x, A) \approx a_3(x) - b_3(x)\cdot |\log(A)| \tag{4}$$

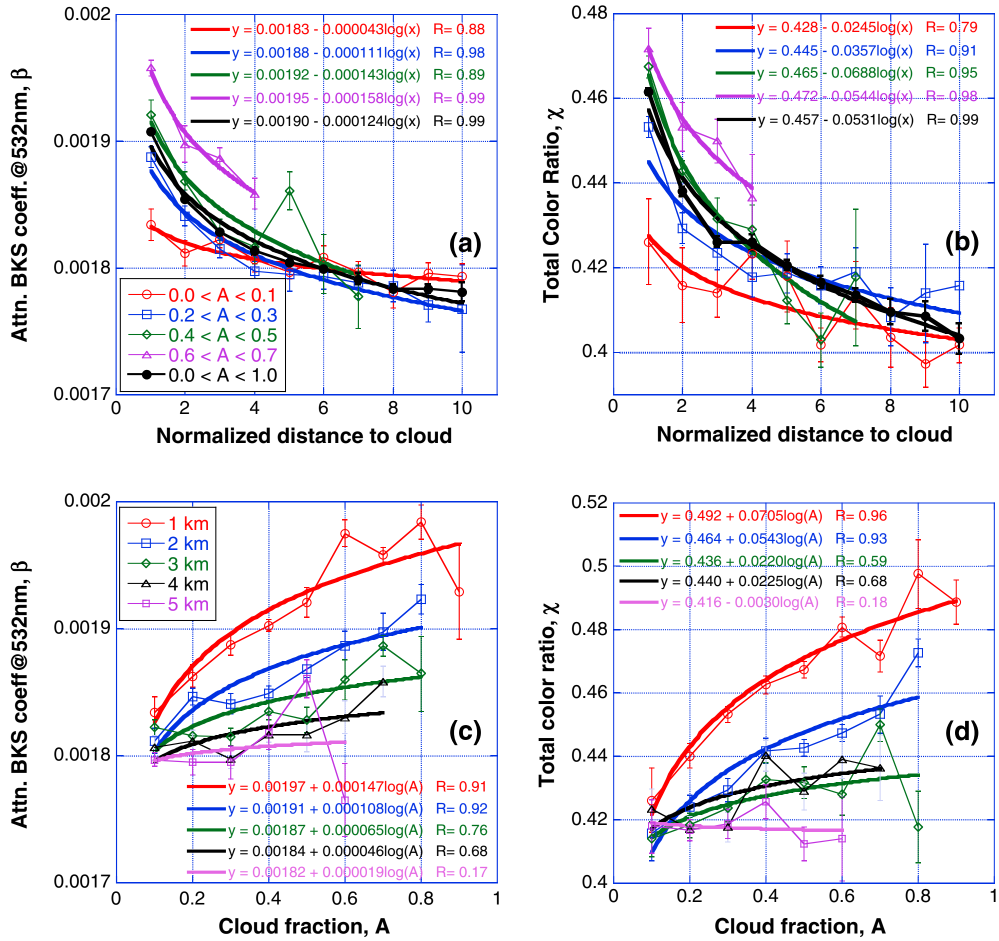

Figure 3. Medians of attenuated total backscatter coefficient β and total color ratio χ as a function of normalized distance to cloud x and cloud fraction A. (a) Median attenuated total backscatter coefficient versus normalized distance to cloud and a log fit: $\beta(x,A) \approx a_1(A) - b_1(A)\cdot\log(x)$ with $x \geq 1$, for four intervals of cloud fraction (0.0–0.1, 0.2–0.3, 0.4–0.5, and 0.6–0.7) and the average one (0.0–1.0). Note that the distance to cloud is normalized by resolution of 1 km and both $a_1(A) = \beta(x=1,A)$ and $b_1(A)$ are increasing functions of A. (b) The same as in Figure 3a but for attenuated total color ratio. Log fits are $\chi(x,A) \approx a_2(A) - b_2(A)\cdot\log(x)$ with $x \geq 1$; $a_2(A) = \chi(x=1,A)$. (c) Median attenuated total backscatter coefficient versus cloud fraction and a log fit: $\beta(x,A) \approx a_3(x) - b_3(x)\cdot|\log(A)|$ with $1 \geq A \geq 0.1$ for five distances to cloud ranging from 1 km to 5 km. Note that both $a_3(x) = \beta(x,A=1)$ and $b_3(A)$ are decreasing functions of x. (d) The same as in Figure 3c but for total color ratio. Log fits are $\chi(x, A) \approx a_4(x) - b_4(x)\cdot|\log(A)|$ with $1 \geq A \geq 0.1$; $a_4(x) = \chi(x,A=1)$. The curves in Figures 3a–3d have been truncated for large distances to clouds and/or large cloud fractions because the sample numbers after the truncated point are either zero or extremely low leading to large uncertainties.

for $x \geq 1$ and $A \geq 0.1$. Here coefficient $a_3(x)$, as a function of x, is equal to the asymptotic value of β if $A = 1$ and $b_3(x)$ describes the degree of cloud fraction dependence for each distance from cloud. We can see that both functions a_3 and b_3 are decreasing; in other words, the bigger the distance from cloud the weaker dependence of aerosol properties on cloud fraction (compare red and magenta curves in Figures 3c or 3d). An approximation similar to equation (4) is also valid for the attenuated total color ratio χ (see Figure 3d).

The presence of near-cloud enhancements for all cloud fractions in Figure 3 confirm that the enhancement in composite statistics comes, at least in part, from physical changes near clouds. Meanwhile, the dependence of $n(x, A)$ on x in Figure 2 indicates that a sampling artifact is also likely to affect the composite statistics (see Figure 1).

In order to estimate the impact of sampling effects on the composite statistics, we resample our data to make the distribution of cloud fraction ($n(x,A)$) used in equation (1) the same for any distance to clouds. We specify this distribution to be the one observed at distance x_0, a large distance beyond which aerosol properties

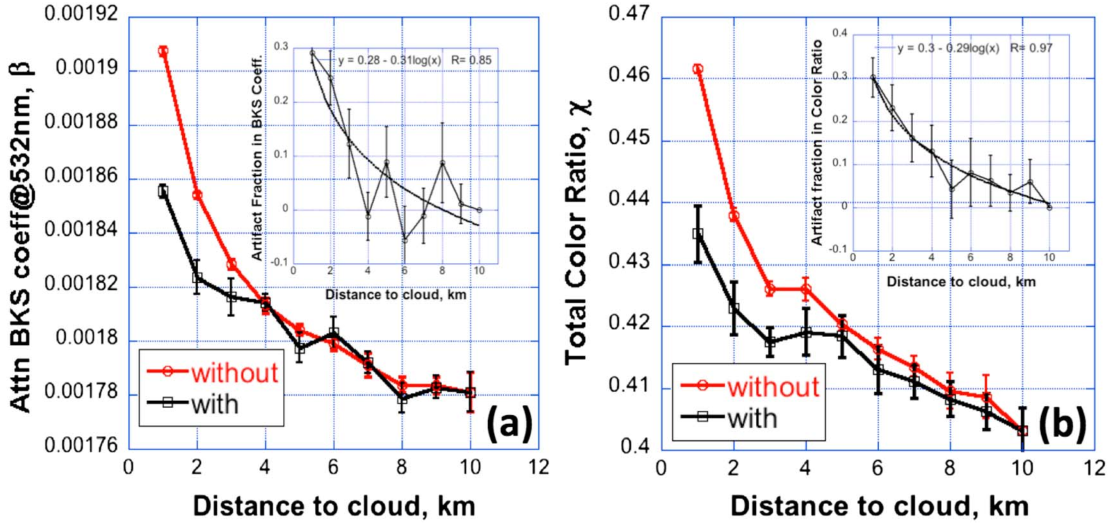

Figure 4. Medians of attenuated total backscatter coefficient and color ratio as a function of distance to cloud without and with removing the sampling effect. Inserts show sampling effect fraction (1-*with*/*without*). (a) Median attenuated total backscatter coefficient. (b) Median attenuated total color ratio.

vary little with cloud fraction. In this study we use $x_0 = 10$ km (Figure 3). This resampling will make the distribution of cloud fraction to be $n(x,A) = n(x_0,A)$ for any $x \geq 1$, thus removing the impacts on composite statistics combining data for all cloud fractions.

Figure 4 compares the β and χ values *with* and *without* applying the proposed resampling method. It shows that near-cloud enhancements become significantly smaller with the resampling (black curves) than they were without the resampling (red curves), and that the differences are mostly within 5 km from clouds. Here the near-cloud enhancement of β and χ is defined as the relative increase over the value at 20 km beyond which aerosols are less affected by clouds [e.g., *Twohy et al.*, 2009]. The inserts show that the fraction of enhancement by the sampling effect also varies with distance to clouds; for this data set it can reach 30% at the distance of 1 km.

It should be noted that the sampling effect depends on location and season. The example technique of using a preselected cloud fraction distribution at a certain far-from-cloud distance (x_0) is not the only method for removing the artifacts caused by near-cloud variations in cloud fraction distributions. The key here is to use identical cloud fraction distributions at all distances, so that the sampling artifact caused by variations in cloud fraction distributions in equation (1) can be removed.

4. Concluding Remarks

Several studies [e.g., *Tackett and Girolamo*, 2009; *Várnai and Marshak*, 2011; *Yang et al.*, 2012; *Várnai et al.*, 2013] have found that aerosol properties vary systematically with distance to the nearest cloud, pointing to the presence of a wide transition zone around clouds. In this paper we examine whether the apparent enhancement of aerosol backscatter and color ratio observed near clouds is indeed a sign of a such transition zone or it is just a manifestation of the well-documented correlation between aerosol properties and cloud fraction [e.g., *Loeb and Manalo-Smith*, 2005; *Chand et al.*, 2012]. This question arises because clear-sky sample populations used in the statistical analysis can be different near clouds and far from clouds: Near-cloud samples are more likely to come from areas/times with higher cloud fractions, while far-from-cloud samples are more likely to come from areas/times of lower cloud fractions.

To answer this question, we analyzed the cloud fraction dependence of near-cloud sample numbers and aerosol optical properties using CALIOP nighttime data from a wide region around the Azores. The results indicate that as expected, near-cloud aerosol statistics are dominated by data for higher cloud fractions, while far-from-cloud statistics are dominated by data for lower cloud fractions. At the same time, however, near-cloud enhancements remain large even if we use samples only from a narrow cloud fraction interval, especially if this cloud fraction is high. In addition, it is found that the cloud fraction dependence of near-cloud behaviors can be well approximated by logarithmic functions (equations (2)–(4)).

These findings indicate that near-cloud aerosol statistics are affected by cloud fraction distributions changing with distance to cloud. The effects can be removed if, for all distances to cloud, we resample the data to the same cloud fraction distribution. When resampling our entire data set to the cloud fraction distribution observed at 10 km away from clouds, the near-cloud enhancement of our original data set was reduced by up to 30%, with most reduction occurring within 5 km from clouds.

This result suggests that systematic changes in the near-cloud transition zone are real but somewhat weaker than previously reported and that understanding the statistics of near-cloud aerosol properties requires a consideration of changes in cloud fraction.

Acknowledgments
We gratefully acknowledge support for this research by the NASA CALIPSO project supervised by Charles Trepte and by the NASA award NNX13AQ35G, as well as the support from the U.S. Department of Energy (DOE) Office of Science (BER) under grants DE-SC0005457 and DE-SC0006865MOD0002. We also thank Alex Kostinski, Alexei Lyapustin, and Larry Di Girolamo for helpful discussions and suggestions. The CALIPSO data were obtained from the NASA Langley Research Center Atmospheric Sciences Data Center.

The Editor thanks an anonymous reviewer for his/her assistance evaluating this paper.

References

Astin, I., L. Di Girolamo, and H. M. van dePoll (2001), Bayesian confidence intervals for true fractional coverage from finite transect measurements: Implications for cloud studies from space, *J. Geophys. Res.*, *106*(D15), 17,303–17,310, doi:10.1029/2001JD900168.

Bar-Or, R. Z., I. Koren, and O. Altaratz (2010), Estimating cloud field coverage using morphological analysis, *Environ. Res. Lett.*, *5*, doi:10.1088/1748-9326/5/1/014022.

Bar-Or, R. Z., O. Altaratz, and I. Koren (2011), Global analysis of cloud field coverage and radiative properties, using morphological methods and MODIS observations, *Atmos. Chem. Phys.*, *11*, 191–200.

Bar-Or, R. Z., I. Koren, O. Altaratz, and E. Fredj (2012), Radiative properties of humidified aerosols in cloudy environment, *Atmos. Res.*, *118*, 280–294.

Cattrall, C., J. Reagan, K. Thome, and O. Dubovik (2005), Variability of aerosol and spectral lidar and backscatter and extinction ratios of key aerosol types derived from selected Aerosol Robotic Network locations, *J. Geophys. Res.*, *110*, D10S11, doi:10.1029/2004JD005124.

Chand, D., R. Wood, S. Ghan, M. Wang, M. Ovchinnikov, P. J. Rasch, S. Miller, B. Schichtel, and T. Moore (2012), Aerosol optical depth enhancement in partly cloudy conditions, *J. Geophys. Res.*, *117*, D17207, doi:10.1029/2012JD017894.

Charlson, R. J., A. S. Ackerman, F. A.-M. Bender, T. L. Anderson, and Z. Liu (2007), On the climate forcing consequences of the albedo continuum between cloudy and clear air, *Tellus*, *59B*, 715–727, doi:10.1111/j.1600-0889.2007.00297.x.

Clarke, A. D., et al. (2002), INDOEX aerosol: A comparison and summary of chemical, microphysical, and optical properties observed from land, ship, and aircraft, *J. Geophys. Res.*, *107*(D19), 8033, doi:10.1029/2001JD000572.

Dong, X., B. Xi, A. Kennedy, P. Minnis, and R. Wood (2014), A 19-month record of marine aerosol–cloud–radiation properties derived from DOE ARM mobile facility deployment at the azores. Part I: Cloud fraction and single-layered MBL cloud properties, *J. Clim.*, *27*, 3665–3682, doi:10.1175/JCLI-D-13-00553.1.

Hoppel, W. A., G. M. Frick, and R. E. Larson (1986), Effect of nonprecipitating clouds on the aerosol size distribution in the marine boundary layer, *Geophys. Res. Lett.*, *13*, 125–128, doi:10.1029/GL013i002p00125.

Ignatov, A., P. Minnis, N. Loeb, B. Wielicki, W. Miller, S. Sun-Mack, D. Tanre, L. Remer, I. Laslo, and E. Geier (2005), Two MODIS aerosol products over ocean on the Terra and Aqua CERES SSF, *J. Atmos. Sci.*, *62*, 1008–1031.

Kassianov, E. I., and M. Ovtchinnikov (2008), On reflectance ratios and aerosol optical depth retrieval in the presence of cumulus clouds, *Geophy. Res. Lett.*, *35*, L06311, doi:10.1029/2008GL033231.

Kaufman, Y. J., and I. Koren (2006), Smoke and pollution aerosol effect on cloud cover, *Science*, *313*, 655–658.

Koren, I., L. A. Remer, Y. J. Kaufman, Y. Rudich, and J. V. Martins (2007), On the twilight zone between clouds and aerosols, *Geophys. Res. Lett.*, *34*, L08805, doi:10.1029/2007GL029253.

Koren, I., J. V. Martins, L. A. Remer, and H. Afargan (2008), Smoke invigoration versus inhibition of clouds over the Amazon, *Science*, *321*, 946–949.

Koren, I., G. Feingold, H. Jiang, and O. Altaratz (2009), Aerosol effects on the inter-cloud region of a small cumulus cloud field, *Geophys. Res. Lett.*, *36*, L14805, doi:10.1029/2009GL037424.

Liu, Z., P. Voelger, and N. Sugimoto (2000), Simulations of the observation of clouds and aerosols with the Experimental Lidar in Space Equipment system, *Appl. Opt.*, *39*, 3120–3137.

Liu, Z., M. A. Vaughan, D. M. Winker, C. A. Hostetler, L. R. Poole, D. Hlavka, W. Hart, and M. McGill (2004), Use of probability distribution functions for discriminating between cloud and aerosol in lidar backscatter data, *J. Geophys. Res.*, *109*, D15202, doi:10.1029/2004JD004732.

Liu, Z., M. Vaughan, D. Winker, C. Kittaka, B. Getzweich, R. Kuehn, A. Omar, K. Powell, C. Trepte, and C. Hostetler (2009), The CALIPSO lidar cloud and aerosol discrimination: Version 2 algorithm and initial assessment of performance, *J. Atmos. Oceanic Technol.*, *26*, 1198–1213.

Loeb, N. G., and G. L. Schuster (2008), An observational study of the relationship between cloud, aerosol and meteorology in broken low-level cloud conditions, *J. Geophys. Res.*, *113*, D14214, doi:10.1029/2007JD009763.

Loeb, N. G., and N. Manalo-Smith (2005), Top-of-atmosphere direct radiative effect of aerosols over global oceans from merged CERES and MODIS observations, *J. Clim.*, *18*, 3506–3526.

Lu, M. L., J. Wang, A. Freedman, H. H. Jonsson, R. C. Flagan, R. A. McClatchey, and J. H. Seinfeld (2003), Analysis of humidity halos around trade wind cumulus clouds, *J. Atmos. Sci.*, *60*, 1041–1059.

Marshak, A., G. Wen, J. A. Coakley Jr., L. A. Remer, N. G. Loeb, and R. F. Cahalan (2008), A simple model for the cloud adjacency effect and the apparent bluing of aerosols near clouds, *J. Geophys. Res.*, *113*, D14S17, doi:10.1029/2007JD009196.

Matheson, M. A., J. A. Coakley Jr., and W. R. Tahnk (2005), Aerosol and cloud property relationships for summertime stratiform clouds in the northeastern Atlantic from AVHRR observations, *J. Geophys. Res.*, *110*, D24204, doi:10.1029/2005JD006165.

Omar, A. H., J.-G. Won, D. M. Winker, S.-C. Yoon, O. Dubovik, and M. P. McCormick (2005), Development of global aerosol models using cluster analysis of Aerosol Robotic Network (AERONET) measurements, *J. Geophys. Res.*, *110*, D10S14, doi:10.1029/2004JD004874.

Omar, A. H., et al. (2009), The CALIPSO automated aerosol classification and lidar ratio selection algorithm, *J. Atmos. Oceanic Technol.*, *26*, 1994–2014, doi:10.1175/2009JTECHA1231.1.

Platt, C. M. R., and D. J. Gambling (1971), Laser radar reflexions and downward infrared flux enhancement near small cumulus clouds, *Nature*, *232*, 182–185.

Qiu, S., G. Godden, X. Wang, and B. Guenther (2000), Satellite-Earth remote sensor scatter effects on Earth scene radiometric accuracy, *Metrologia*, *37*, 411–414.

Redemann, J., Q. Zhang, P. B. Russell, J. M. Livingston, and L. A. Remer (2009), Case studies of aerosol remote sensing in the vicinity of clouds, *J. Geophys. Res.*, *114*, D06209, doi:10.1029/2008JD010774.

Rémillard, J., P. Kollias, E. Luke, and R. Wood (2012), Marine boundary layer cloud observations at the Azores, *J. Clim.*, *25*, 7381–7398.

Su, W., G. L. Schuster, N. G. Loeb, R. R. Rogers, R. A. Ferrare, C. A. Hostetler, J. W. Hair, and M. D. Obland (2008), Aerosol and cloud interaction observed from high spectral resolution lidar data, *J. Geophys. Res.*, *113*, D24202, doi:10.1029/2008JD010588.

Tackett, J. L., and L. D. Girolamo (2009), Enhanced aerosol backscatter adjacent to tropical trade wind clouds revealed by satellite-based lidar, *Geophys. Res. Lett.*, *36*, L14804, doi:10.1029/2009GL039264.

Twohy, C. H., J. A. Coakley Jr., and W. R. Tahnk (2009), Effect of changes in relative humidity on aerosol scattering near clouds, *J. Geophys. Res.*, *114*, D05205, doi:10.1029/2008JD010991.

Várnai, T., and A. Marshak (2011), Global CALIPSO observations of aerosol changes near clouds, *IEEE Rem. Sens. Lett.*, *8*, 19–23.

Várnai, T., and A. Marshak (2012), Analysis of co-located MODIS and CALIPSO observations near clouds, *Atmos. Meas. Tech.*, *5*, 389–396, doi:10.5194/amt-5-389-2012.

Várnai, T., A. Marshak, and W. Yang (2013), Multi-satellite aerosol observations in the vicinity of clouds, *Atmos. Chem. Phys.*, *13*, 3899–3908, doi:10.5194/acp-13-3899-2013.

Wen, G., A. Marshak, R. F. Cahalan, L. A. Remer, and R. G. Kleidman (2007), 3-D aerosol-cloud radiative interaction observed in collocated MODIS and ASTER images of cumulus cloud fields, *J. Geophys. Res.*, *112*, D13204, doi:10.1029/2006JD008267.

Winker, D. M., W. Hunt, and M. McGill (2007), Initial performance assessment of CALIOP, *Geophys. Res. Lett.*, *34*, L19803, doi:10.1029/2007GL030135.

Wood, R. (2009), Clouds, Aerosol, and Precipitation in the Marine Boundary Layer (CAP-MBL), DOE/SC-ARM-0902, 23 pp. [Available at http://www.arm.gov/publications/programdocs/doe-sc-arm-0902.pdf?id594.]

Wood, R., et al. (2014), Clouds, aerosol, and precipitation in the marine boundary layer: An ARM mobile facility deployment, *Bull. Am. Meteorol. Soc.*, doi:10.1175/BAMS-D-13-00180.1.

Yang, W., A. Marshak, T. Várnai, and Z. Liu (2012), Effect of CALIPSO cloud aerosol discrimination (CAD) confidence levels on observations of aerosol properties near clouds, *Atmos. Res.*, *116*(15), 134–141, doi:10.1016/j.atmosres.2012.03.013.

Zhang, J., J. S. Reid, and B. N. Holben (2005), An analysis of potential cloud artifacts in MODIS over ocean aerosol optical thickness product, *Geophys. Res. Lett.*, *32*, L15803, doi:10.1029/2005GL023254.